Optica Applicata, Vol. XLVI, No. 4, 2016
DOI: 10.5277/oa160407

Simultaneous measurement of refractive index and thickness for optically transparent object with a dual-wavelength quantitative technique

XIAOQING XU[1, 2], YAWEI WANG[1, 3*], YUANYUAN XU[1], WEIFENG JIN[1]

[1]School of Mechanical Engineering, Jiangsu University, Zhenjiang 212013, China

[2]School of Mechanical Engineering, Yangzhou Polytechnic College, Yangzhou 225009, China

[3]Faculty of Science, Jiangsu University, Zhenjiang 212013, China

[*]Corresponding author: jszjwyw@sina.cn

We present a new dual-wavelength quantitative measurement approach that can be employed for simultaneously measuring both the refractive index and the thickness of the homogenous specimen. This method is realized by dual-wavelength in-line phase-shifting digital holography, and then the phase images are obtained by using four-phase step algorithm for each wavelength separately. Based on computer simulation technology, the feasibility and the effectiveness of our proposed method are demonstrated by comparing our simulation results with the experimental results of the spherical silica bead and the red blood cell, respectively. Our work will provide some guidance in the experimental research for transparent phase objects.

Keywords: digital holography, phase measurement, cell measurement, red blood cell.

1. Introduction

Dual-wavelength digital holography (DWDH) not only maintains the advantages of single-wavelength digital holography, such as high sensitivity, high accuracy and non -intrusive method without injury [1, 2], but can yield a synthetic beat wavelength phase by the simple subtraction between two wrapped phases of single-wavelength [3–5]. Recently, DWDH has attracted wide attention in engineering and biology, and then various DWDH techniques have been presented [3–14]. In order to perform a millimeter contouring of the object, DWDH was first introduced by WAGNER *et al*. [7] by subtraction of two reconstructed phase maps obtained with a scanning dye laser. And then, KIM and co-workers proposed a similar technique within the framework of digital holographic microscopy to remove the phase ambiguity of digitally-propagated wavefronts [3, 4]. Additionally, to perform surface height measurements of the sample at the beat wavelength, based on polarizing separation, dual-wavelength in-line and off-axis

digital holographic methods have been presented by ABDELSALAM *et al*. [8, 9] by the application of the flat fielding method.

Generally, the measured phase shift depends on the thickness and the refractive index of a transparent object. To decouple these two parameters, there are two main methods. One is to combine holography-based quantitative phase microscopy with other microscopy techniques, such as diffraction phase microscopy [14], confocal microscopy [15], and tomographic phase microscopy [16]. Since these additional techniques require a mechanical scanning process, the combing method is more complicated. The other is to separate anticipant information from the two phase maps [12, 17], which are obtained from experiments where two types of surrounding solutions with different refractive indices are utilized for the same cell.

In this paper, in order to separately measure the refractive index and the thickness from the quantitative phase images of the optically transparent specimen, a new dual -wavelength quantitative (DWQ) technique is presented based on in-line phase-shifting DWDH. Our DWQ technique is based on the assumption that the refractive index of the phase object cannot be affected by the wavelengths in our experiment. The phase images are acquired by using four-step phase-shifting algorithm for each wavelength separately in in-line phase-shifting DWDH. We illustrate the proposed approach with theory, and prove our method with experimental results of the spherical silica bead and the red blood cell, respectively, by computer simulation technology. In addition, the accuracy of refractive index measurement by our DWQ technique depends on the accuracy of the refractive index in our simulation. The current simulation can provide some guidance for the experimental parameters setting and data processing of transparent phase objects by our DWQ technique.

2. Method of dual-wavelength quantitative technique

The DWQ technique is based on in-line phase-shifting DWDH supplemented by DWQ analysis. As is known, phase-shifting requires at least three images and in general the more images the better the results. For this sake, four-step phase-shifting algorithm is employed to separately obtain both amplitude and phase information of the object at each wavelength. The intensities in the four fringe patterns can be expressed as

$$I_{j+1}(x,y) = I_{\mathrm{o}} + I_{\mathrm{r}} + 2\sqrt{I_{\mathrm{o}} I_{\mathrm{r}}}\cos\left(\varphi_i + \frac{j\pi}{2}\right) \tag{1}$$

where I_{o} and I_{r} are the intensities of the object and the reference waves, respectively, φ_i is the phase corresponding to wavelength λ_i (i = 1, 2), and j is the number of the phase-shifted frames (j = 0 to 3). The phase distribution φ_i corresponding to λ_i using the four-phase step algorithm can be described by

$$\varphi_i = \tan^{-1}\left(\frac{I_4 - I_2}{I_1 - I_3}\right) \tag{2}$$

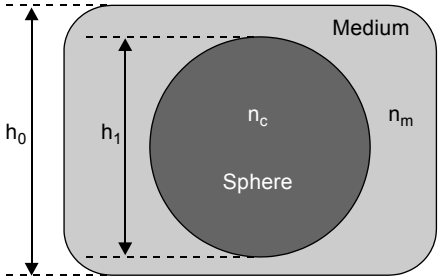

Fig. 1. Schematic of a sphere in a medium.

Suppose that the object is a sphere of thickness h_1 in the optical axis direction, as shown in Fig. 1. The sphere is immersed in the solution with thickness of h_0. The refractive indices of the sphere and the surrounding medium are respectively set to n_{c,λ_i} and n_{m,λ_i} corresponding to λ_i. The index differences of the medium and phase object are defined as $\Delta n_0 = n_{m,\lambda_1} - n_{m,\lambda_2}$ and $\Delta n_c = n_{c,\lambda_1} - n_{c,\lambda_2}$, respectively. With a highly dispersive surrounding, Δn_c can be assumed to be zero for $\Delta n_c \ll \Delta n_0$ in our experiment. Therefore, our DWQ technique is based on the assumption that the refractive index n_c of the phase object cannot be affected by the two wavelengths.

Then, the phase δ_i induced by the specimen corresponding to λ_i can be expressed by

$$\delta_i = \frac{2\pi}{\lambda_i}\left[(n_{m,\lambda_i} - 1)h_0 + (n_c - n_{m,\lambda_i})h_1\right] \tag{3}$$

Removing the reference value $2\pi(n_{m,\lambda_i} - 1)h_0/\lambda_i$, which can be conveniently measured anywhere outside the object, the phase shifting induced by the sphere can be described by

$$\varphi_i = \frac{2\pi}{\lambda_i}(n_c - n_{m,\lambda_i})h_1 \tag{4}$$

In the above equation, n_c and h_1 are unknown and can be obtained by solving Eq. (4) at each wavelength, respectively. Subsequently, the refractive index n_c and the thickness h_1 of the phase object can be simultaneously derived by

$$n_c = n_{m,\lambda_1} + \frac{n_{m,\lambda_1} - n_{m,\lambda_2}}{\lambda_2\varphi_2/(\lambda_1\varphi_1) - 1} \tag{5}$$

$$h_1 = \frac{\lambda_2\varphi_2 - \lambda_1\varphi_1}{2\pi(n_{m,\lambda_1} - n_{m,\lambda_2})} \tag{6}$$

3. Numerical simulations

According to the method, the refractive index and the thickness of the homogenous object can be measured simultaneously from the phase maps, which were obtained by

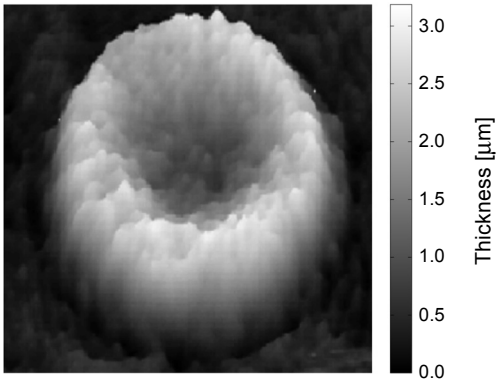

Fig. 2. The thickness distribution of the RBC from [16].

DWQ technique. To demonstrate the applicability and the reliability of this approach, simultaneous measurements of the refractive indices and the thicknesses for the spherical silica bead and the simulated red blood cell (RBC) are investigated using the simulation method, respectively.

In our experiment, a homogenous spherical silica bead and a simulated RBC are used as the imaged objects. The refractive indices of the sphere, with the diameter of 10 μm, are set to $n_{c_1,\lambda_1} = 1.461$ and $n_{c_1,\lambda_2} = 1.457$ at $\lambda_1 = 532$ nm and $\lambda_2 = 632$ nm, respectively. The sphere is immersed in the ethylene glycol, whose indices were $n_{m_1,\lambda_1} = 1.45$ and $n_{m_1,\lambda_2} = 1.43$ for $\lambda_1 = 532$ nm and $\lambda_2 = 632$ nm, respectively. For the spherical silica, Δn_c can be assumed to be zero for $\Delta n_c = 0.004 \ll \Delta n_m = 0.02$. The thickness distribution of the simulated RBC is obtained from [16], as shown in Fig. 2. RBC can be seen as a homogenous object due to the absence of intracellular organelles such as the nucleus and so on, thus the refractive indices are the same in any regions of a RBC. The RBC is immersed in a certain perfusion chamber, whose indices were set to $n_{m_2,\lambda_1} = 1.34$ and $n_{m_2,\lambda_2} = 1.33$ for $\lambda_1 = 488$ nm and $\lambda_2 = 532$ nm. Suppose that the refractive index of RBC cannot be affected by the two wavelengths, thus its refractive index can be seen as a constant. Consequently, the index difference of the RBC Δn_c is zero, which is much less than $\Delta n_m = 0.01$. In addition, to simplify the calculation, the refractive indices of the sphere and the simulated RBC for each wavelength are 1.461 and 1.397, respectively. Both the reference wave and sample wave are considered as plane waves, and their amplitudes are assumed to be 1.

4. Results and discussion

4.1. Spherical silica bead

To verify the applicability of this method, a spherical silica bead has been considered as the experimental sample. With the ethylene glycol medium of refractive index $n_{m_1,\lambda_1} = 1.45$ and $n_{m_1,\lambda_2} = 1.43$, we obtain the phase images of the sphere for $\lambda_1 = 532$ nm and $\lambda_2 = 632$ nm, as exhibited in Figs. 3**a** and 3**b**, respectively. By using

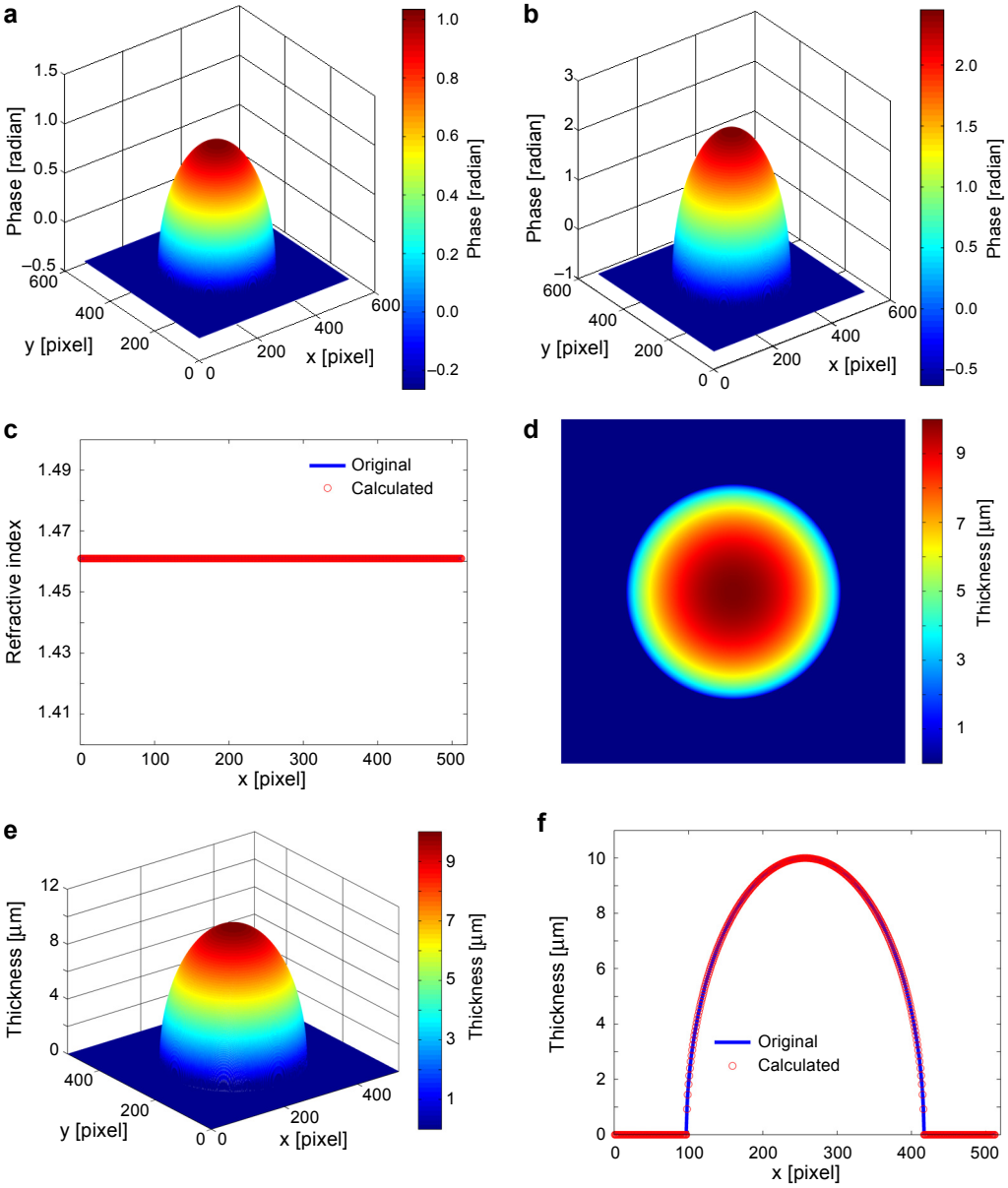

Fig. 3. The spherical silica bead. Phase maps for λ_1 = 532 nm (**a**) and λ_2 = 632 nm (**b**). The calculated refractive index and the original one (**c**). The 2D (**d**) and 3D (**e**) thickness distribution maps. The central horizontal profiles of **d** and the original one (**f**).

Eqs. (5) and (6), the refractive index and the thickness 2D distribution of the sphere can be simultaneously measured based on DWQ technique, as shown in Figs. 3**c** and 3**d**, respectively. From Fig. 3**c**, one can find that the calculated refractive index 1.461 matches the original one very well. Figure 3**e** is the 3D representation of Fig. 3**d**, in

which the shape of the spherical silica bead can be seen clearly. For comparison, the central horizontal profiles of the original and the calculated thickness maps of the spherical silica bead are exhibited in Fig. 3**f**, which shows that the calculated thickness curve (circle) almost agrees with the original thickness curve (solid line). Through the analysis, the measured maximum thickness is 9.9996 μm, and the thickness deviation is 0.0004 μm, which is possibly caused by the phase shifting algorithm that can introduce the detuning errors [18], compared to the original value.

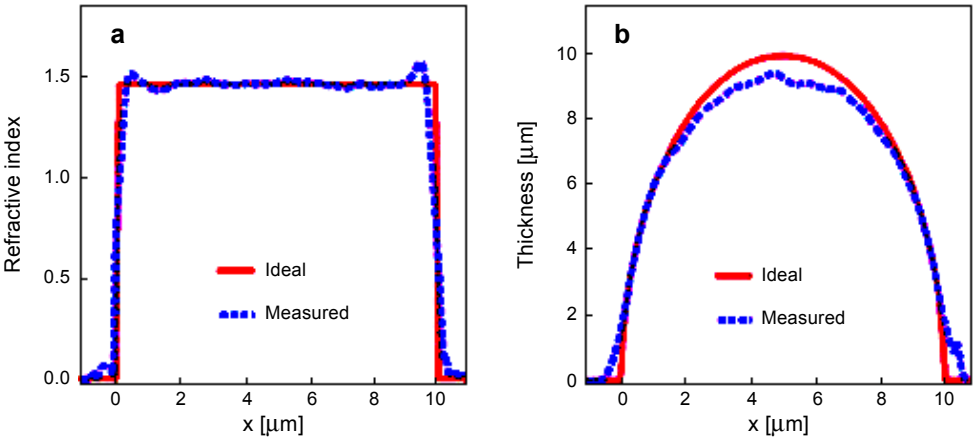

Fig. 4. The spherical silica bead. Experiment results of refractive index (**a**) and thickness (**b**) from [14].

In addition, under the same experimental parameters, from Figs. 3**c** and 3**d**, we can find that our calculated results of the refractive index and the thickness for the spherical silica bead are similar to the experimental ones from JAFARFARD obtained by dual-wavelength diffraction phase microscopy [14], as presented in Figs. 4**a** and 4**b**, respectively. It is noteworthy to mention that the whole work can be carried out by the MATLAB software.

4.2. Red blood cell

To experimentally demonstrate that DWQ technique is suitable for the quantitative measurement of the biological specimen, we have applied this algorithm to measure both the refractive index and the thickness of the simulated RBC. With the medium of refractive index $n_{m_2,\lambda_1} = 1.34$ and $n_{m_2,\lambda_2} = 1.33$, the phase images of the simulated RBC for $\lambda_1 = 488$ nm and $\lambda_2 = 532$ nm are obtained, respectively, as presented in Figs. 5**a** and 5**b**. By using DWQ technique, we can simultaneously acquire both the refractive index and the thickness distribution of RBC based on Eqs. (5) and (6), as shown in Figs. 5**c** and 5**d**, respectively. From Fig. 5**c**, one can find that the calculated refractive index 1.397 almost agrees with the original one. Comparing Fig. 5**d** with the original thickness distribution image shown in Fig. 2, one can see that there is no

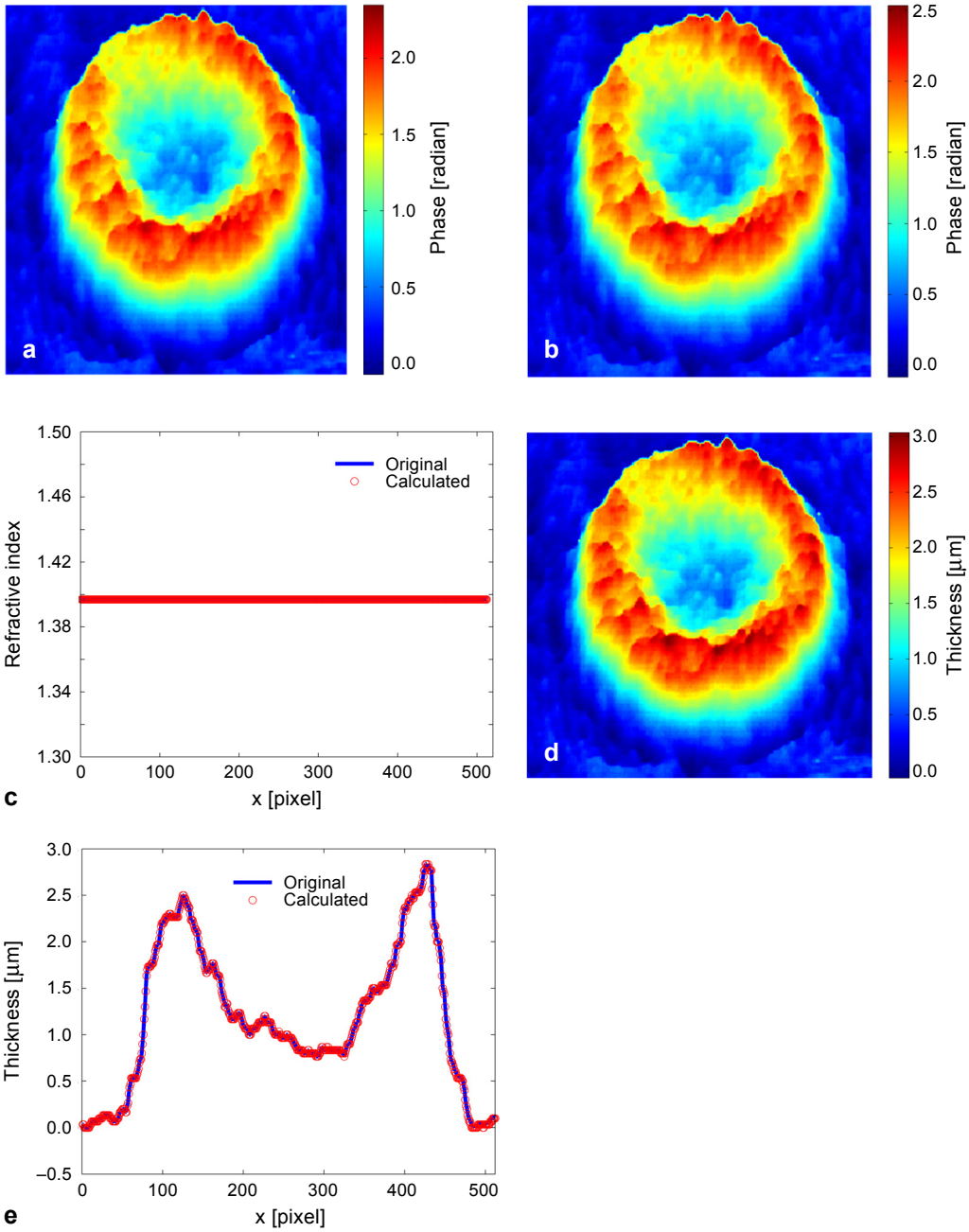

Fig. 5. The simulated RBC. Phase maps for $\lambda_1 = 488$ nm (**a**) and $\lambda_2 = 532$ nm (**b**). The calculated refractive index and the original one (**c**). The thickness distribution map (**d**). The horizontal profiles of **d** and the original one (**e**).

significant difference between them. For further comparison to demonstrate the accuracy of this approach, the profiles of the original and the calculated physical thickness maps of RBC in the horizontal row are presented in Fig. 5**e**, which illustrates the fact that the calculated thickness curve (circle) and the original thickness curve (solid line) are almost superimposed, meaning that the DWQ technique is valid for simultaneously measuring both the refractive indices and the thicknesses of biological cells.

5. Conclusions

In summary, a new DWQ technique based on in-line phase-shifting DWDH has been presented in this paper. By using the simulation method, the results show that both the calculated refractive indices and the calculated thicknesses of the spherical silica bead and the RBC agree well with the original ones, respectively. Compared to the original value, the thickness deviation is 0.0004 μm for the spherical silica bead. The profile of the original thickness matches the calculated one very well for RBC. The applicability and reliability of DWQ technique have been verified by our work. Therefore, our work will take a significant role in the experimental research on transparent objects. In addition, our work will also provide a technical support for simultaneous measurement of both the refractive index and the thickness for biological specimen.

Acknowledgements – This work was supported by National Natural Science Foundation of China (Nos. 11374130, 11474134 and 11604127) and the Doctoral Program Joint Fund of Colleges and Universities Specialized Research (No. 20113227110018).

References

[1] GOODMAN J.W., LAWRENCE R.W., *Digital image formation from electronically detected holograms*, Applied Physics Letters **11**(3), 1967, pp. 77–79.

[2] KÜHN J., COLOMB T., MONTFORT F., CHARRIÈRE F., EMERY Y., CUCHE E., MARQUET P., DEPEURSINGE C., *Real-time dual-wavelngth digital holographic microscopy with a single hologram acquisition*, Optics Express **15**(12), 2007, pp. 7231–7242.

[3] GASS J., DAKOFF A., KIM M.K., *Phase imaging without 2π ambiguity by multiwavelength digital holography*, Optics Letters **28**(13), 2003, pp. 1141–1143.

[4] PARSHALL D., KIM M.K., *Digital holographic microscopy with dual-wavelength phase unwrapping*, Applied Optics **45**(3), 2006, pp. 451–459.

[5] KHMALADZE A., MYUNG KIM, CHUN-MIN LO, *Phase imaging of cells by simultaneous dual-wavelength reflection digital holography*, Optics Express **16**(15), 2008, pp. 10900–10911.

[6] YEOU-YEN CHENG, WYANT J.C., *Two-wavelength phase shifting interferometry*, Applied Optics **23**(24), 1984, pp. 4539–4543.

[7] WAGNER C., OSTEN W., SEEBACHER S., *Direct shape measurement by digital wavefront reconstruction and multiwavelength contouring*, Optical Engineering **39**(1), 2000, pp. 79–85.

[8] ABDELSALAM D.G., MAGNUSSON R., DAESUK KIM, *Single-shot, dual-wavelength digital holography based on polarizing separation*, Applied Optics **50**(19), 2011, pp. 3360–3368.

[9] ABDELSALAM D.G., DAESUK KIM, *Two-wavelength in-line phase-shifting interferometry based on polarizing separation for accurate surface profiling*, Applied Optics **50**(33), 2011, pp. 6153–6161.

[10] KUMAR U.P., BASANTA BHADURI, KOTHIYAL M.P., KRISHNA MOHAN N., *Two-wavelength micro-interferometry for 3-D surface profiling*, Optics and Lasers in Engineering **47**(2), 2009, pp. 223–229.

[11] Barada D., Kiire T., Sugisaka J., Kawata S., Yatagai T., *Simultaneous two-wavelength Doppler phase-shifting digital holography*, Applied Optics **50**(34), 2011, pp. H237–H244.

[12] Rappaz B., Charrière F., Depeursinge C., Magistretti P.J., Marquet P., *Simultaneous cell morphometry and refractive index measurement with dual-wavelength digital holographic microscopy and dye-enhanced dispersion of perfuson medium*, Optics Letters **33**(7), 2008, pp. 744–746.

[13] Hee Joo Choi, Hwan Hong Lim, Han Seb Moon, Tae Bong Eom, Jung Jin Ju, Myoungsik Cha, *Measurement of refractive index and thickness of transparent plate by dual-wavelength interference*, Optics Express **18**(9), 2010, pp. 9429–9434.

[14] Jafarfard M.R., Sucbei Moon, Behnam Tayebei, Dug Young Kim, *Dual-wavelength diffraction phase microscopy for simultaneous measurement of refractive index and thickness*, Optics Letters **39**(10), 2014, pp. 2908–2911

[15] Niyom Lue, Wonshik Choi, Popescu G., Zahid Yaqoob, Kamran Badizadegan, Dasari R.R., Feld M.S., *Live cell refractometry using Hilbert phase microscopy and confocal reflectance microscopy*, The Journal of Physical Chemistry A **113**(47), 2009, pp. 13327–13330.

[16] Popescu G., YoungKeun Park, Wonshik Choi, Dasari R.R., Feld M.S., Badizadegan K., *Imaging red blood cell dynamics by quantitative phase microscopy*, Blood Cells, Molecules, and Diseases **41**(1), 2008, pp. 10–16.

[17] Rappaz B., Marquet P., Cuche E., Emery Y., Depeursinge C., Magistretti P.J., *Measurement of the integral refractive index and dynamic cell morphometry of living cells with digital holographic microscopy*, Optics Express **13**(23), 2005, pp. 9361–9373.

[18] Mosiño J.F., Servin M., Estrada J.C., Quiroga J.A., *Phasorial analysis of detuning error in temporal phase shifting algorithms*, Optics Express **17**(7), 2009, pp. 5618–5623.

Received February 1, 2016
in revised form May 11, 2016